EPR characterization of the mononuclear Cu-containing *Aspergillus japonicus* quercetin 2,3-dioxygenase reveals dramatic changes upon anaerobic binding of substrates

Ingeborg M. Kooter[1,*,†], **Roberto A. Steiner**[2,†], **Bauke W. Dijkstra**[2], **Paula I. van Noort**[1], **Maarten R. Egmond**[1] and **Martina Huber**[3]

[1]*Unilever Research Vlaardingen, the Netherlands;* [2]*University of Groningen, Laboratory of Biophysical Chemistry, Groningen, the Netherlands;* [3]*Department of Molecular Physics, Leiden University, the Netherlands*

Quercetin 2,3-dioxygenase (2,3QD) is a copper-containing dioxygenase that catalyses the oxidation of the flavonol quercetin to 2-protocatechuoylphloroglucinol carboxylic acid with concomitant production of carbon monoxide. In contrast to iron dioxygenases, very little is known about copper dioxygenases. We have characterized 2,3QD from the fungus *Aspergillus japonicus* by electron paramagnetic resonance spectroscopy (EPR). At pH 6.0, 2,3QD shows a mixture of two EPR species. The major form has parameters typical of type 2 Cu sites ($g_{//} = 2.330$, $A_{//} = 13.7$ mT), the minor one has a more distorted geometry ($g_{//} = 2.290$, $A_{//} = 12.5$ mT). Anaerobic addition of the substrate quercetin results in a different, single species EPR spectrum with $g_{//} = 2.336$, $A_{//} = 11.4$ mT, parameters, which are in-between those of the type 2 and type 1 Cu sites in the Peisach–Blumberg ($g_{//}$ vs. $A_{//}$) plot. After turnover, a new EPR signal is observed, which is ascribed to the carboxylic acid ester product complex. This spectrum is similar to that of the native enzyme at pH 10.0 and has *g*-tensor parameters suggesting a trigonal bipyramidal site. Of a variety of flavonoids studied, only flavonols are able to bind to the copper centre of 2,3QD. Nine flavonols with different hydroxylation patterns at the A- and B-ring have been analysed. They cluster in two different regions of the Peisach–Blumberg plot and show that the presence of a 5-OH group has a large effect on the $A_{//}$ parameter. Several differences are noted between *A. japonicus* 2,3QD and the enzyme from *A. niger* German Collection of Microorganisms 821.

Keywords: electron paramagnetic resonance; dioxygenase; quercetin; copper.

Dioxygenases are enzymes that use molecular oxygen to oxidize their substrates by incorporating both oxygen atoms into the reaction product. These enzymes play an important role in the biosynthesis and catabolism of various types of metabolites and in several detoxification mechanisms [1]. Dioxygenases are mostly metalloproteins [2]. Nonhaem iron is the prosthetic group commonly employed, and iron-containing dioxygenases have been widely studied [3,4]. In contrast, less information is available on copper-containing dioxygenases.

In 1971, it was reported that quercetin 2,3-dioxygenase (2,3QD) from *Aspergillus flavus* is a 111-kDa organic cofactor devoid copper-dependent dioxygenase containing two moles of copper per mole of enzyme [5]. The enzyme is heavily glycosylated (27.5%, w/w). Under aerobic conditions it catalyses the conversion of the flavonoid quercetin (3′,4′,5,7-tetrahydroxyflavonol) to the corresponding depside (phenolic ester 2-protocatechuoylphloroglucinol carboxylic acid) and carbon monoxide (Fig. 1) [6]. This reaction is rather unusual in that it involves the cleavage of two carbon–carbon bonds and the concomitant production of carbon monoxide. The stoichiometry of the process is such that 2 mol of substrate are converted per mol of enzyme, that is, 1 mol of substrate per mol of copper, consistent with the later finding of a homo-dimeric protein.

Recently, 2,3QD from *Aspergillus niger* German Collection of Microorganisms 821 has been reported as a 148-kDa glycoprotein (sugar content 46–54%, w/w) containing 1.0–1.6 mol of Cu [7] per mol of protein. The enzyme is composed of three different subunits with molecular masses of 63–67, 53–57, and 31–35 kDa, respectively, organized in a 1 : 1 : 1 quaternary structure. *Aspergillus niger* DSM 821 has been characterized by EPR spectroscopy. It shows parameters of a nonblue type 2 Cu^{2+} protein ($g_{//} = 2.293$ and $A_{//} = 15.5$ mT). A resolved multiline pattern of at least nine resonances in the perpendicular region has been tentatively assigned to an interaction of the copper ion with four nitrogen ligands in a distorted square-planar geometry. Addition of the substrate quercetin under anaerobic

Fig. 1. Reaction catalyzed by 2,3QD.

Fig. 3. Schematic representation of a possible mechanism of 2,3QD-mediated dioxygenation of flavonols. Adapted from [9].
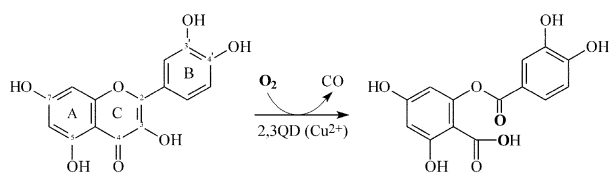
conditions in a threefold molar excess did not yield any spectral effects, leaving the native spectrum unaltered.

The first direct structural information on a 2,3QD enzyme became available only recently [8]. The crystal structure of 2,3QD from *Aspergillus japonicus* (hereafter, unless explicitly stated, 2,3QD will indicate the enzyme from this source) solved at pH 5.2 and 1.6 Å resolution shows that the enzyme is a glycoprotein homodimer (sugar content $\approx 25.0\%$, w/w) of about 100 kDa containing one atom of copper per monomer (350 amino acids). The crystallo-graphic analysis reveals that the copper centre of 2,3QD has two alternative conformations (Fig. 2). The main form ($\approx 70\%$ of the total) is pseudo-tetrahedral and derives from the ligation of three histidine residues (His66, His68 and His112) and a water molecule (Wat1 in Fig. 2). The minor coordination form ($\approx 30\%$) has a mixed trigonal bipyram-idal/square pyramidal geometry where the copper is coordinated by the same three histidine residues, a water molecule (Wat2 in Fig. 2) and the Glu73 side chain. The latter residue coordinates the metal only in its minor conformation. In its principal conformation the carboxylate side chain of Glu73 points away from the metal centre.

Though precise mechanistic information on 2,3QD-mediated dioxygenation of flavonols is lacking, the early biochemical study on *A. flavus* 2,3QD and primarily several bio-mimetic studies [9–13] have suggested the general features of a possible mechanism for the enzymatic reaction (Fig. 3). The first step is believed to be the binding of the flavonol substrate to the copper ion (structure **2** in Fig. 3). Subsequently, an activated complex (**3**) is assumed to be attacked either at C2 or at the Cu^+ ion by the dioxygen molecule. The oxygenated complexes (not shown) would then form through different routes, and the endoperoxide (**4**) decomposes to release the products (**5**) and regenerate

the native enzyme (**1**). This mechanism is based on that of intradiol dioxygenases, which utilize high-spin Fe(III) in place of copper [3].

Here, we report EPR studies of 2,3QD that characterize the native enzyme, the anaerobic complexes with nine different flavonol substrates, and the depside bound enzyme forms. Our study offers the first EPR description of important catalytic states of the dioxygenation process of flavonols and shows that the anaerobic binding of flavonols produces clear changes in the electronic distribution at the copper centre.

EXPERIMENTAL PROCEDURES

Cloning of 2,3QD

Aspergillus japonicus IFO-4408 was grown in media con-taining 6 g·L^{-1} NaNO$_3$, 2 g·L^{-1} KH$_2$PO$_4$, 5 g·L^{-1} fructose, 1 g·L^{-1} MgSO$_4$·7H$_2$O, Egli trace elements (per L: 0.6 g EDTA·2H$_2$O, 0.11 g CaCl$_2$·2H$_2$O, 75 mg FeSO$_4$·7H$_2$O, 28 mg MnSO$_4$·H$_2$O, 27 mg ZnSO$_4$·7H$_2$O, 8 mg CuSO$_4$· 5H$_2$O, 9 mg CoCl$_2$·6H$_2$O, 5 mg Na$_2$MoO$_4$·2H$_2$O, 8 mg H$_3$BO$_3$, 5 mg KI, pH 4.0 with NaOH), 0.1–0.5% yeast extract and quercetin (10 g·L^{-1}). 2,3QD was purified from the culture broth (100-L fermentation, 0.4 mg·L^{-1}) and the N-terminal amino-acid sequence was determined and used to synthesize two degenerate primers (5′-CKIGCRTGIS WRTARTG-3′) and (5−GAYACIWSIWSIYTIATYGTI GARGAYGCICC-3′). A PCR reaction on *A. japonicus* genomic DNA with the primers resulted in a 77-bp fragment encoding the N-terminal end of the enzyme. This PCR fragment was used in a colony hybridization on a *A. japonicus* genomic library in pBluescript. A hybridizing colony was identified, cultivated and plasmid DNA was isolated. Sequence analyses showed that the sequence is 1200-bp long, encoding a protein of 379 amino acids with one intron of 63 base-pairs; this was confirmed by PCR on cDNA and subsequent sequence analysis of the cloned fragment. 2,3QD is most likely synthesized as a prepro-enzyme, containing a putative presequence of 18 amino acids (according to the predictions by Von Heijne [14,15]), and a pro-sequence of 10 amino acids, followed by a mature protein of 351 amino acids.

Production of 2,3QD

For the production and secretion of 2,3QD by the mould *Aspergillus awamori*, the complete 2,3QD encoding
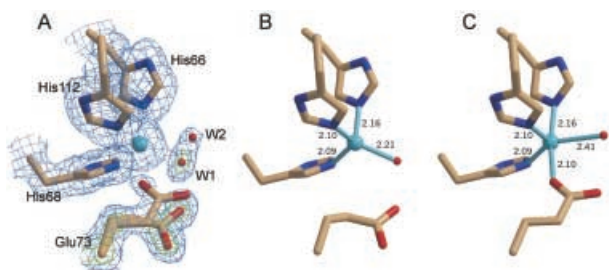

Fig. 2. Copper coordination geometries in 2,3QD. (A) Experimental $2F_o–F_c$ map contoured at the 1.0 σ (blue) and 2.5 σ (green, only for Glu73 and the solvent molecule) levels. (B) Major distorted tetrahedral coordination. (C) Minor trigonal bipyramidal coordination with a strong square pyramidal component. In (B) and (C) the coordination distances are reported in Å. This figure was generated with the programs BOBSCRIPT [26] and RASTER3D [27].
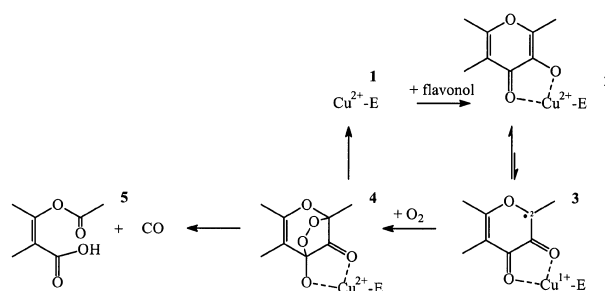
sequence (including signal-sequence) was cloned between the endoxylanase promoter and transcription terminator in the *Aspergillus* expression vector pAW14B-12, resulting in the plasmid pUR7857. Strain *Aspergillus awamori* was cotransformed with a 5.7-kb *Sal*I fragment from pUR7857 (containing an exact fusion between 2,3QD and the *Aspergillus awamori* endoxylanase promoter and transcription terminator) and a 2.4-kb *Bam*HI–*Hin*dIII fragment from pAW4-1 containing the *A. awamori pyrG* gene as selection marker. Transformants were screened for extracellular production of 2,3QD in a plate-screening assay. Plates containing 6 g·L^{-1} NaNO$_3$, 2 g·L^{-1} KH$_2$PO$_4$, 1 g·L^{-1} MgSO$_4$·7H$_2$O, Egli trace elements, 0.5% yeast extract, 1% D-xylose, 1.5% agar and 1% quercetin were inoculated with spores obtained from the transformants and incubated at 30 °C. Transformants that produced a halo i.e. a clear zone of bleached quercetin were purified twice and finally spores were isolated on potato dextrose agar (Oxoid) plates. Cultivation of a recombinant *Aspergillus awamori* strain in a fermenter resulted in 2,3QD levels of ≈ 0.3 g·L^{-1}.

Purification of 2,3QD

The recombinant 2,3QD was purified from the culture broth as follows. The first step involved a 60% ammonium sulfate precipitation, after which the solution was centrifuged for 30 min at 25 000 *g*. The soluble fraction was then dialysed against 50 mM Mes pH 6.0 and loaded on a DEAE–Sepharose fast flow column (Pharmacia), and eluted at 300 mM NaCl. After concentration the enzyme was loaded on a Superdex 200 gel filtration column and eluted with 50 mM Mes pH 6.0 and 100 mM NaCl. The enzyme activity was measured as described previously by Oka *et al.* [16]. One unit was defined as the amount of enzyme that converts 1 μmol of quercetin per min at 25 °C. The standard assay (1 mL) contained 50 mM Mes buffer pH 6.0, 20 μL of 3 mM quercetin (dissolved in dimethylsulfoxide) and 10 μL enzyme solution. The specific activity of the final purified preparation was typically 90 U·mg^{-1}. The Cu content of the enzyme is 0.8 mol·(mol protein)$^{-1}$ (per monomer), as determined by atomic absorption spectroscopy. The analysis was performed by plasma emission spectrometry using a PerkinElmer Models Plasma 1000.

EPR measurements

X-Band EPR measurements were performed with a Bruker ECS 106 EPR spectrometer. Samples were placed into quartz tubes and frozen in liquid nitrogen. Spectra were acquired with EPR tubes in a liquid nitrogen-containing finger dewar (at 77 K) using a power of 2 mW. In general, the spectra were obtained as 3-min scans from 210 to 410 mT using a time constant of 0.3 s, a modulation amplitude of 1.27 mT, and a field modulation frequency of 50 kHz. Measurements were generally carried out at pH 6.0 in 50 mM Mes buffer. This pH value was chosen because it is close to the pH of maximum enzymatic activity (pH 6.2, M. van der Heiden, unpublished results) and matches the conditions generally employed in the enzymatic activity assay [7,16]. The measurement at pH 10.0 was carried out in an universal buffer system containing 25 mM citric acid, 25 mM potassium dihydrogen phosphate, 25 mM boric acid, 25 mM tricine adjusted to the desired pH value with NaOH.

Anaerobic measurements were performed on samples prepared using an in-house built argon-vacuum flush system.

The flavonoids (quercetin, kaempferol, myricetin, morin, datiscetin, galangin, 3OH-flavone, 3,7(OH)$_2$-flavone, fisetin) were obtained from Fluka, Sigma, Aldrich or Roth and dissolved in dimethylsulfoxide. Diethyldithiocarbamate (DDC) was dissolved in water prior to its use.

Determination of EPR parameters

For all species, EPR parameters were read directly from the line positions as shown in Fig. 4A. For selected spectra, simulations with the program SIMFONIA (Bruker Analytische Messtechnik GmbH) were performed. Uncertainties of the EPR parameters obtained by simulation were estimated according to the sensitivity of the spectra to the
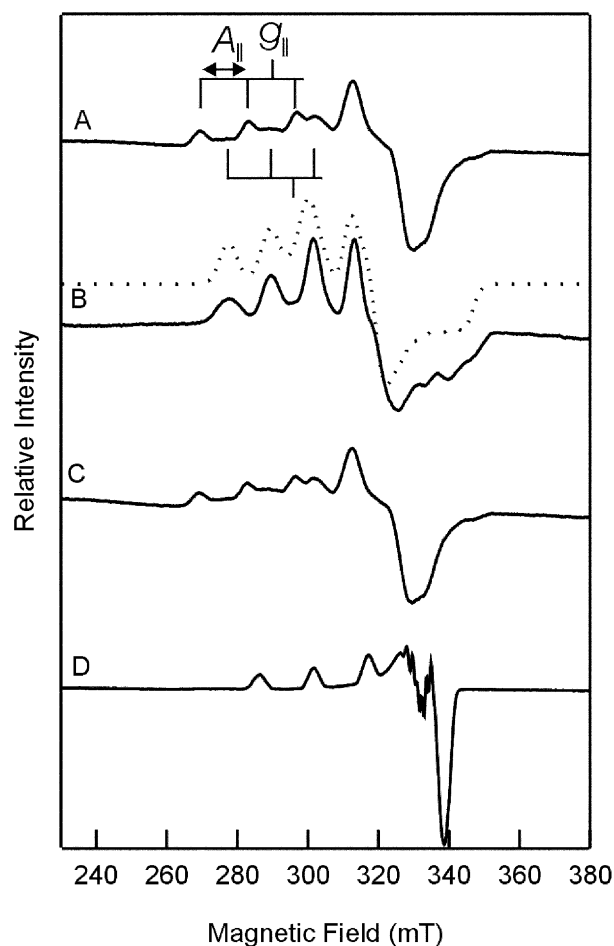

Fig. 4. EPR spectra of 2,3QD. (A) 2,3QD in 50 mM Mes buffer, pH 6.0; (B) 2,3QD in universal buffer, pH 10.0 (C) 2,3QD sample of spectrum (B), after the pH has been brought back to pH 6.0; (D) DDC-inhibited 2,3QD in 50 mM Mes buffer, pH 6.0. In (A), the positions of the lines used to read off the EPR parameters of the major and the minor species are shown. Dotted line (B) Simulation of EPR spectrum at pH 10.0; parameters, see text. Simulation did not take into account a possible variation of the line widths of lines belonging to different nuclear magnetic quantum numbers (m$_I$), which explains part of the differences between the experimental and simulated spectra.

respective parameter. No calibration of absolute g values was performed, but an estimate of the absolute error in g values was obtained from comparing the g values of DPPH measured on separate occasions, which were between 2.0053 and 2.0063 [Lit: 2.0037(2)] [17]. This suggests that the absolute g values have an error of ± 0.0013, which is negligible in the present context.

RESULTS AND DISCUSSION

Native 2,3QD at pH 6.0 and pH 10.0

The EPR spectrum of native 2,3QD at pH 6.0 is presented in Fig. 4A. The spectrum clearly indicates that the purified enzyme contains two different EPR species, a major and a minor one. The EPR parameters are $g_{//}$ and $A_{//}$ values of 2.330 and 13.7 mT, and 2.290 and 12.5 mT for the major and minor form, respectively. The locations of both forms (yellow circles) in the Peisach–Blumberg plot [18] are shown in Fig. 5. Whereas the major form possesses EPR parameters close to those of a type 2 Cu site, that is, relatively large $g_{//}$ and $A_{//}$ values, and a g-tensor of nearly axial symmetry, with $g_{//} > g_{\perp}$, the minor form has a smaller $A_{//}$ value indicating a more distorted site [19]. Increasing the pH from 6.0 to 10.0 changes the spectrum to that of a single EPR species (Fig. 4B), with $g_{//} = 2.289$ and $A_{//} = 11.7$ mT (magenta circle in Fig. 5). This change is fully reversible since lowering the pH again to 6.0 results in the original spectrum (Fig. 4C). As the spectral line-shape of the spectrum at pH 10 differs significantly from that expected for a typical type 2 copper site a simulation was performed.

The simulation of the EPR spectrum of 2,3QD at pH 10.0 is shown in Fig. 4. The simulation parameters are $g_{zz} = 2.289(4)$, $g_{yy} = 2.178(5)$, $g_{xx} = 2.011(3)$, $A_{zz} = 12.0(2)$ mT, and A_{xx}, $A_{yy} = 6.0(3)$ mT, where g_{zz} and A_{zz} correspond to the observed $g_{//}$ and $A_{//}$ values, respectively. The parameters read off from the spectrum are thus in

good agreement with the results of the simulation. Remarkable are the large hyperfine couplings A_{xx} and A_{yy}, and the ordering of the g values, both of which differ from those expected for type 2 copper sites. For example, the g_{zz} and g_{yy} values are much closer to each other, indicating a substantial perturbation of the axial symmetry of the tensor, whereas axial symmetry, i.e. $g_{xx} \approx g_{yy} << g_{zz}$ is typically found for type 2 sites. The grouping of the g-values and the line-shape of the spectrum at pH 10.0 are similar to those reported for Cu^{2+} in model complexes [20–22], where they are attributed to trigonal bipyramidal species.

The simulated EPR spectrum at pH 10.0 has characteristics that are close to the resolved features of the minor species in the native enzyme spectra at pH 6.0. The difference in $A_{//}$ values of 6% can be attributed to uncertainties in determining the line-position of the minor species at pH 6.0, caused by the superposition of spectra at this pH value. Comparison of the high-field region, where absorptions due to g_{xx} and g_{yy} occur, is hampered by the spectral overlap with the major species in this region, but overall, the similarity of the line-shape and of $g_{//}$ and $A_{//}$ suggests that the minor pH 6.0 species is similar, if not identical, to the high pH form. Assuming that the remaining EPR parameters of the minor species, in particular the g-tensor components, are similar to those of the species observed at pH 10, the minor species would have a lower symmetry than the major species, and EPR parameters suggestive of a trigonal bipyramidal geometry [20–22].

To correlate the EPR results to the two crystallographically observed forms is difficult, as the two coordinations are too irregular to be mapped onto the geometries of model complexes, which presently provide the only way in which structural aspects can be derived from EPR parameters. A possible interpretation would be to identify the major crystallographic coordination with the (according to the g-tensor parameters) more (axially) symmetric major EPR species and the minor coordination to the more distorted, possibly trigonal bipyramidal, minor EPR species. Although in this interpretation, the relative intensities of the two forms in the X-ray structure and the EPR spectra agree, we are aware that a number of factors may influence these ratios: differences in pH and physical state between the EPR and crystallographic samples, presence of additives in the crystallization mixture, difference in temperature, crystal packing and manner of freezing, and the use of different preparations and batches. Nevertheless, EPR spectroscopy and X-ray crystallography agree beyond doubt on the existence of a mixed coordination at the cupric centre of 2,3QD at functionally relevant pH values.

Diethyldithicarbamate-inhibited 2,3QD

Diethyldithiocarbamate (DDC) is a known chelating agent for copper and a strong inhibitor of 2,3QD. In Fig. 4D, the EPR spectrum of the DDC-inhibited enzyme at pH 6 is reported. This compound drastically changes the EPR spectrum of 2,3QD, giving rise to a single EPR signal with $g_{//}$ and $A_{//}$ values of 2.182 and 15.5 mT (cyan circle in Fig. 5), respectively. The lowering of the $g_{//}$ value is indicative of sulfur ligation to the copper-site. The recently solved X-ray structure of the DDC-inhibited 2,3QD [23] confirms this and shows that the enzyme is penta coordi-
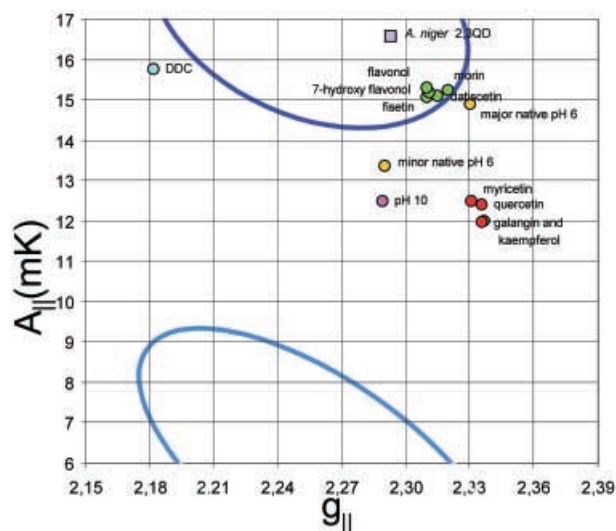
Fig. 5. Peisach–Blumberg plot. Plot of $g_{//}$ and $A_{//}$ values from EPR of the various flavonol complexes, as read off from the spectra, see also Table 1. Parameters of additional complexes are reported in the text. Area circled in dark blue: the region where type 2 Cu sites in proteins are found; light blue, where type 1 sites are found, according to [18].

nated with a regular square pyramidal geometry where the copper is ligated by His66, His68, His112 and the two sulfur atoms of DDC.

Anaerobic complexation of 2,3QD with its natural substrate quercetin

Anaerobic incubation of 2,3QD with quercetin (5,7,3′,4′-tetrahydroxy flavonol dissolved in dimethylsulfoxide) at pH 6.0 resulted in a totally new and single species EPR signal (Fig. 6A) characterized by $g_{//}$ and $A_{//}$ values of 2.336 and 11.4 mT (red circle in Fig. 5). Comparison of this
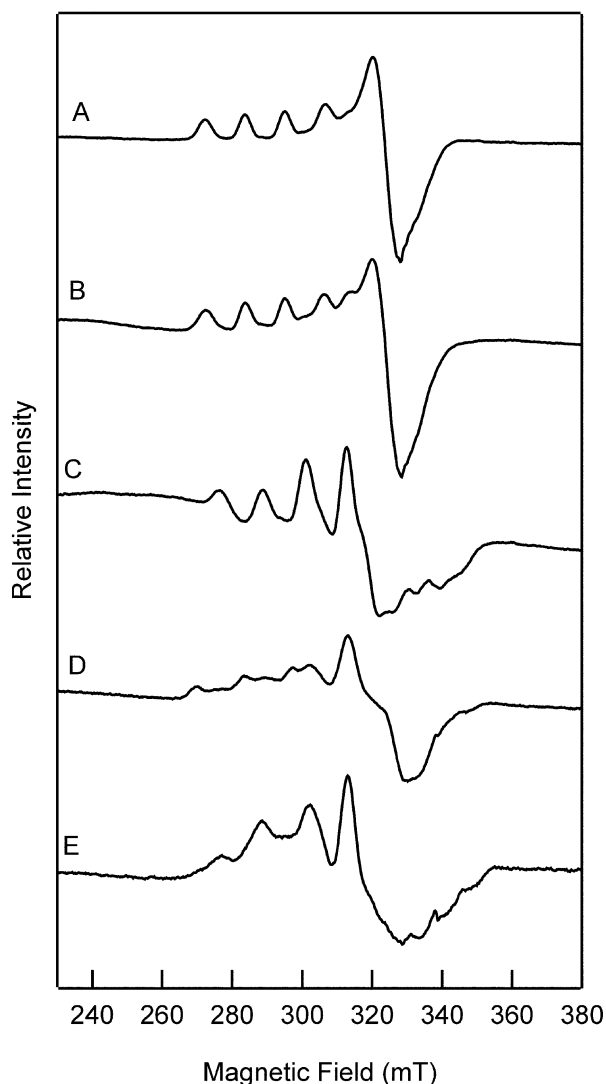

Fig. 6. EPR spectra of quercetin and depside bound 2,3QD. (A) 2,3QD·quercetin (1 : 1 molar ratio, 2.5% dimethylsulfoxide v/v, pH 6.0). (B) 2,3QD·quercetin (1 : 1 molar ratio, quercetin added as a solid, pH 6.0). (C) Sample (A) after addition of oxygen (air). (D) Sample (C) after four cycles of concentration and dilution with 50 mM Mes buffer, pH 6.0 in an YM10 concentrator (Amicon Inc., Danvers, MA, USA) to remove molecules of molecular mass lower than 10 kDa. (E) aerobically prepared 2,3QD·depside (2-protocatechuoyl-phloroglucinol carboxylic acid, twofold excess) complex in 50 mM Mes buffer, pH 6.0 (the spectrum has been corrected for the presence of some native enzyme).

spectrum with that from a sample prepared by anaerobic addition of solid quercetin to the enzyme solution (Fig. 6B) indicates that the changes observed in the former are entirely due to the presence of quercetin, and are not affected significantly by the solvent DMSO. Quantification of the total spin concentration from the EPR signals from the spectra of Fig. 4A (native form) and 6A (quercetin bound form) resulted in values of 0.78 and 0.85 spins per monomer, respectively, which agrees with the copper content of 0.8 mol copper per mol of protein found from atomic absorption spectroscopy measurements, indicating that no large scale reduction of copper takes place upon substrate ligation.

It was already reported by Oka *et al.* [6] that upon anaerobic incubation with *A. flavus* 2,3QD, flavonols that serve as substrates undergo a bathochromic shift in their UV/vis spectra. With quercetin, for example, the visible flavonolic band shifted from 367 to 380 nm [6]. As flavonols are known to absorb at longer wavelengths upon complex formation with metals [24], the red shift was taken as evidence that flavonols interact with the metal centre prior to dioxygen attack. The EPR spectrum of 2,3QD incubated with quercetin in the absence of dioxygen is consistent with this hypothesis. The presence of the natural substrate causes specific changes in the electronic environment of 2,3QD that are interpreted in terms of the formation of an enzyme·flavonol complex. As a result of the small hyperfine splitting this copper centre falls in a region of the Peisach–Blumberg plot in between those usually occupied by type 2 and type 1 Cu sites (Fig. 5).

Turn-over conditions

Exposure to oxygen (air) of the 2,3QD samples incubated with quercetin (either dissolved in dimethylsulfoxide or added as a solid) yielded an EPR spectrum (Fig. 6C), different from that of the native enzyme (Fig. 4A). Thus, after the oxygenation reaction has taken place, the enzyme returns to a state that is different from the original one. To investigate this in more detail, the sample after turn-over was extensively washed with 50 mM Mes, pH 6.0, by repeated concentrations and dilutions. This resulted in the original spectrum of the native enzyme (Fig. 6D), indicating that most likely a bound reactant had been removed. Aerobic addition to the native enzyme of 2-protocatechuoyl-phloroglucinol carboxylic acid in twofold excess resulted in the EPR spectrum shown in Fig. 6E. Except for an admixture of a small contribution of a native like EPR spectrum, the spectrum in Fig. 6E is similar to the EPR spectrum of the enzyme after turnover (Fig. 6C) whereas addition of CO (under saturation conditions) did not affect the EPR spectrum (not shown). Therefore, we conclude that the differences in the spectrum are to be ascribed to the depside product, which remains bound to the copper centre after turn-over.

Interestingly, the EPR parameters obtained from simulations of the spectrum after turnover (Fig. 6C) are similar to those of the pH 10.0 native species discussed above [$g_{zz} = 2.295(4)$, $g_{yy} = 2.169(5)$, $g_{xx} = 2.014(3)$, $A_{zz} = 12.2(2)$ mT, $A_{yy} = 4.2(2)$ mT, and $A_{xx} = 6.7(3)$ mT]. Hence, we expect the complex after turnover to be similar to the native enzyme at high pH, i.e. having a distorted trigonal bipyramidal structure.

Binding of different flavonols

In addition to quercetin, eight flavonols (galangin, kaempferol, myricetin, morin, datiscetin, fisetin, 7-hydroxy flavonol and flavonol) (see Table 1 for their structures) have been studied in this work. Similarly to what was observed in the presence of its natural substrate, anaerobic incubation at pH 6.0 of 2,3QD with each of them produced well-defined spectra (Fig. 7) characterized by the $g_{//}$ and $A_{//}$ parameters reported in Table 1. Figure 5 shows the location of each of these $g_{//}$, $A_{//}$ couples in the Peisach–Blumberg plot (red and green circles).

The various complexes cluster in two regions of the $g_{//}$–$A_{//}$ plane 2,3QD complexes with quercetin, kaempferol, myricetin and galangin (red circles) have $g_{//}$ values ranging from 2.331 to 2.337, rather small $A_{//}$ parameters (11.0–11.5 mT) and fall in a region intermediate to those where type 1 and type 2 Cu sites are usually found. The remaining complexes (green circles) display marginally lower $g_{//}$ (2.310–2.320) and higher $A_{//}$ (14.0–14.2 mT) parameters. They are clustered in a region of the Peisach–Blumberg plot generally occupied by type 2 sites and close to where the major native EPR form is located. All spectra have an overall line-shape of an approximately axially symmetric g-tensor, similar to that of the quercetin bound complex, suggesting the arrangement of copper ligands to be similar for all substrate bound complexes.

Overall, it seems that variations in flavonol structure affect $A_{//}$ more than $g_{//}$. Whereas the range of $g_{//}$ covered in the various complexes is rather limited (2.310–2.337), $A_{//}$ varies considerably ranging from 11.0 to 14.2 mT. The presence of a 5-OH group appears to have particularly large effects on the electronic structure of the copper centre, driving $A_{//}$ to low values. Though the exact reason for this is not clear, we speculate that it might be related to the hydrogen bond, which is formed between the carbonyl oxygen at the C-ring and the 5-OH proton when the latter substituent is present. Such a bond is expected to increase the positive polarization of the C4 atom and to influence through mesomeric effects the electronic distribution at the copper centre.

Interestingly, the presence of a 2′-OH group in the B-ring counterbalances the effect produced by the presence of 5-OH whereas other OH substitutions at the B-ring have no effect. The only explanation for this effect appears to be related to the abnormally low pK_a of the 2′-OH (≈ 3.5) group [25]. At pH 6.0, morin and datiscetin bear a negative charge, which is delocalized over the π-electron system of the substrate. With respect to the $g_{//}$ and $A_{//}$ parameters, this seems to compensate the effect induced by the 5-OH group, producing $g_{//}$ and $A_{//}$ parameters similar to those of compounds substituted at less influential positions.

Flavonol specificity

The specificity of 2,3QD for flavonol binding has been tested by anaerobically incubating the enzyme with different flavonoids. The addition of a flavone (apigenin), of a flavanonol (taxifolin) and of a flavan-3-ol (epicatechin) (Fig. 8) did not alter the EPR spectra of the enzyme indicating the absence of binding to the copper centre. From the chemical structures of the tested flavonoids we conclude

that the presence of a free 3-OH group and an overall planar molecular structure are strict requirements for binding to the 2,3QD active site. This result agrees with what is expected from the shallow shape of the active site cleft observed in the X-ray structure [8].
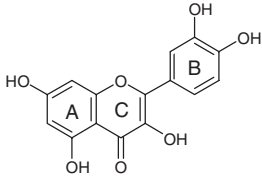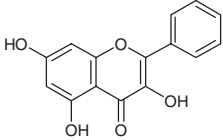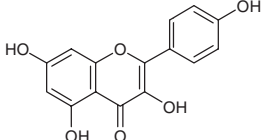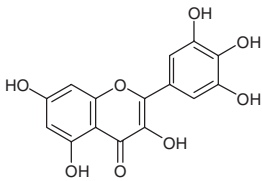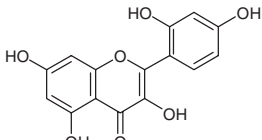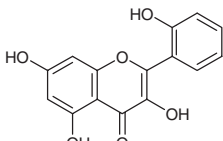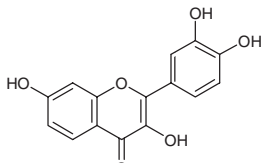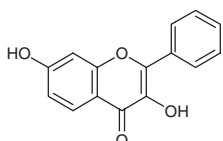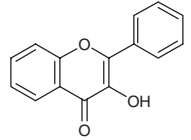
Comparison with *A. niger* DSM 821 2,3QD

A. niger DSM 821 2,3QD is the only other 2,3QD characterized by EPR [7]. The main differences between 2,3QD and *A. niger* DSM 821 2,3QD are that in the latter (a) a single species EPR spectrum of the enzyme in the native state ('as isolated') is observed, with (b) EPR parameters ($g_{//} = 2.293$ and $A_{//} = 15.5$ mT), that differ significantly from 2,3QD (major species: $g_{//} = 2.330$ and $A_{//} = 13.7$ mT, see also respective location on Blumberg–Peisach plot, Fig. 5). From the EPR results, it was proposed (c) that in *A. niger* DSM 821 2,3QD, the metal interacts with four nitrogen residues resulting in a distorted square planar copper centre [7], whereas in 2,3QD a coordination of copper to three histidines plus water and/or Glu73 is found by X-ray crystallography. Differences in copper ligation of the two enzymes are consistent with (a) and (b), but further interpretation is difficult, as for *A. niger* DSM 821 2,3QD neither the amino-acid sequence nor the X-ray structure are known. Also (d), in *A. niger* DSM 821 2,3QD no changes in the EPR spectra were observed upon anaerobic addition of a threefold molar excess of quercetin [7]. Owing to the ease with which flavonols form complexes with copper, (d) suggests that the copper site in *A. niger* DSM 821 2,3QD is not accessible to the substrate under anaerobic conditions. The combination of these factors suggests that the reaction mechanism of the two enzymes differs significantly, which is not too surprising given that the quaternary structure of *A. niger* DSM 821 2,3QD seems to be different from that of 2,3QD [7]. Of particular interest is the fact that from (a) and (b), it could be concluded that there is no residue like Glu73 in *A. niger* DSM 821 2,3QD. In 2,3QD Glu73 is probably responsible for the complex EPR spectrum of the native 2,3QD and it seems to be required for function, since mutation of Glu73 with other natural amino acid resulted only in virtually inactive variants (I. M. Kooter *et al.* unpublished). We hope that additional studies will be carried out on *A. niger* DSM 821 2,3QD in order to further investigate this seemingly very different system.

CONCLUSIONS

The results of this EPR study on *A. japonicus* quercetin 2,3-dioxygenase are consistent with an enzymatic mechanism similar to that presented in Fig. 3, and permit a more precise definition of some of the catalytic steps. Binding of the various flavonols to the active site metal centre is found not to require the presence of dioxygen and occurs without formal reduction of the cupric centre (structure **2** in Fig. 3). This therefore indicates that the activated state **3** is, at least in absence of dioxygen, not highly populated suggesting that the equilibrium between **2** and **3** strongly favours the former. Model studies with $[Cu^{2+}(fla)(idpa)]ClO_4$ [fla = flavonolate, idpa = 3,3′-imino-bis(*N*,*N*-dimethylpropylamine)] [13] agree with this. Whereas details on dioxygen attack and on the steps immediately following it

Table 1. List of studied flavonols and relative $g_{//}$ and $A_{//}$ values.

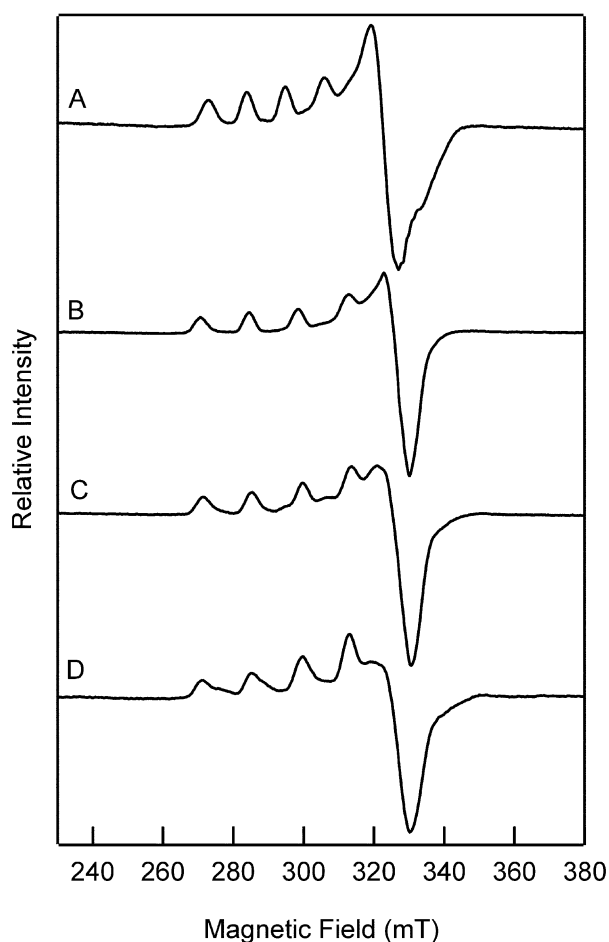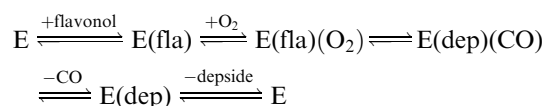| Compound	Chemical structure	OH pattern at rings A and B	$g_{//}$ and $A_{//}$ (mT)
Quercetin		5,7; 3′,4′	2.336; 11.4
Galangin		5,7; none	2.337; 11.0
Kaempferol		5,7; 4′	2.336; 11.0
Myricetin		5,7; 3′,4′,5′	2.331; 11.5
Morin		5,7; 2′,4′	2.320; 14.1
Datiscetin		5,7; 2′	2.315; 14.0
Fisetin		7; 3′,4′	2.310; 14.0
7-Hydroxy flavonol		7; none	2.311; 14.1
Flavonol (3-hydroxy flavone)		none; none	2.310; 14.2

Fig. 7. EPR spectra of other anaerobic 2,3QD·flavonol complexes.
(A) 2,3QD·kaempferol. (B) 2,3QD·morin. (C) 2,3QD·fisetin. (D) 2,3QD·flavonol. All spectra were recorded at pH 6.0 (50 mM Mes buffer) with a flavonol to enzyme ratio of 1 : 1 (2,3QD concentration was ≈ 0.84 mM). Dimethylsulfoxide concentration in the samples was 2.5% (v/v).
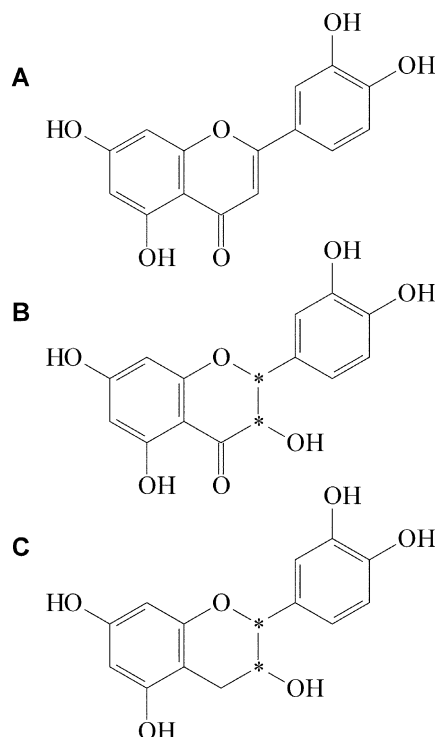

Fig. 8. Chemical structure of tested flavonoids. (A) the flavone apigenin. (B) the flavanonol taxifolin. (C) the flavan-3-ol epicatechin. The asterisks indicate the stereocentres. In the cases of (B) and (C) racemic mixtures were used.

are still largely obscure, the formation after turn-over of the E·depside complex might indicate that the product carbon monoxide leaves the metal centre prior to the depside. Schematically, the reaction might therefore proceed as follows:

$$E \underset{\xrightarrow{\text{+flavonol}}}{} E(\text{fla}) \underset{\xrightarrow{\text{+O}_2}}{} E(\text{fla})(O_2) \rightleftharpoons E(\text{dep})(CO)$$

$$\underset{\xleftarrow{-CO}}{\rightleftharpoons} E(\text{dep}) \underset{\xrightarrow{-\text{depside}}}{\rightleftharpoons} E$$

More work has clearly to be carried out on this very intriguing class of dioxygenases in order to fully elucidate how the copper centre is exploited in the enzymatic reaction.

ACKNOWLEDGEMENTS

REFERENCES

1. Hayaishi, O. (1974) General Properties and Biological Functions of Oxygenases. In *Molecular Mechanisms of Oxygen Activation* (Hayaishi, O., ed.), pp. 1–28. Academic Press, New York.
2. Bairoch, A. (1993) The ENZYME database. *Nucleic Acids Res.* **21**, 3155–3156.
3. Que, L. Jr (1999) Oxygen Activation at Nonheme Iron Centers. In *Bioinorganic Catalysis* (Reedijk, J. & Bouwman, E., eds), pp. 269–321. Marcel Dekker, Inc., New York.
4. Broderick, J.B. (1999) Catechol dioxygenases. *Essays Biochem.* **34**, 173–189.
5. Oka, T. & Simpson, F.J. (1971) Quercetinase, a dioxygenase containing copper. *Biochem. Biophys. Res. Commun.* **43**, 1–5.
6. Oka, T., Simpson, F.J. & Krishnamurty, H.G. (1972) Degradation of rutin by *Aspergillus flavus*. Studies on specificity, inhibition, and possible reaction mechanism of quercetinase. *Can. J. Microbiol.* **18**, 493–508.
7. Hund, H.K., Breuer, J., Lingens, F., Huttermann, J., Kappl, R. & Fetzner, S. (1999) Flavonol 2,4-dioxygenase from *Aspergillus niger* DSM 821, a type 2 Cu(II)-containing glycoprotein. *Eur. J. Biochem.* **263**, 871–878.
8. Fusetti, F., Schröter, K.H., Steiner, R.A., van Noort, P.I., Pijning, T., Rozeboom, H.J., Kalk, K.H., Egmond, M.R. & Dijkstra, B.W. (2002) Crystal structure of the copper-containing quercetin 2,3-dioxygenase from *Aspergillus japonicus*. *Structure* **10**, 259–268.
9. Speier, G. (1991) Quercetin 2,3-dioxygenase mimicking chemistry. In *Dioxygen Activation and Homogeneous Catalytic Oxidation*

(Simándi, L.I., ed.), pp. 269–278. Elsevier Science Publishers B.V., Amsterdam.

10. Balogh-Hergovich, E., Kaizer, J. & Speier, G. (2000) Kinetics and mechanism of the Cu(I) and Cu(II) flavonolate-catalyzed oxygenation of flavonol. Functional quercetin 2,3-dioxygenase models. *J. Mol. Cat.* **159**, 215–224.

11. Kaizer, J. & Speier, G. (2001) Radical-initiated oxygenation of flavonols by dioxygen. *J. Mol. Cat.* **171**, 33–36.

12. Barhács, L., Kaizer, J. & Speier, G. (2001) Kinetics and mechanism of the stoichiometric oxygenation of the ionic zinc (II) flavonolate complex [Zn (fla) (idpa)]ClO4 (fla=flavonolate; idpa=3,3′-iminobis (*N*,*N*-dimethylpropylamine). *J. Mol. Catal.* **172**, 117–125.

13. Barhács, L., Kaizer, J., Pap, J. & Speier, G. (2001) Kinetics and mechanism of the stoichiometric oxygenation of [Cu (II) (fla) (idpa)]ClO4 [fla = flavonolate, idpa = 3,3′-iminobis (N,N-dimethylpropylamine)] and the [Cu (II) (fla) (idpa)]ClO4-catalysed oxygenation of flavonol. *Inorg. Chim. Acta* **320**, 83–91.

14. Von Heijne, G. (1985) Signal sequences – The limits of variation. *J. Mol. Biol.* **184**, 99–105.

15. Von Heijne, G. (1986) A new method for predicting signal sequence cleavage sites. *Nucleic Acids Res.* **14**, 4863–4690.

16. Oka, T., Simpson, F.J., Child, J.J. & Mills, C. (1971) Degradation of rutin by *Aspergillus flavus*. Purification of the dioxygenase quercetinase. *Can. J. Microbiol.* **17**, 111–118.

17. Weil, J.A., Bolton, J.R. & Wertz, J.E. (1994) Appendix E 3. Measurement of g-and hyperfine parameters. In *Electron Paramagnetic Resonance*, p. 511. John Wiley & Sons Inc, New York.

18. Peisach, J. & Blumberg, W.E. (1974) Structural implications derived from the analysis of electron paramagnetic resonance spectra of natural and artificial copper proteins. *Arch. Biochem. Biophys.* **165**, 691–708.

19. Vanngård, T. (1972) Copper proteins. In *Biological Applications of Electron Spin Resonance* (Swartz, H.M., Bolton, J.R. & Borg, D.C., eds), pp. 411–447. John Wiley & Sons, Inc., New York.

20. Addison, A.W., Hendriks, H.M.J., Reedijk, J. & Thompson, L.K. (1981) Copper complexes of the tripod tris (2-benzimidazolylmethyl) amine-5-coordinate and 6-coordinate copper(II) derivatives and some copper(I) derivatives. *Inorg. Chem.* **20**, 103–110.

21. Jiang, F., Karlin, K.D. & Peisach, J. (1993) An electron-spin echo envelope modulation (ESEEM) strudy of electron-nuclear hyperfine and nuclear–quadrupole interactions of d_z^2 ground-state copper(II) complexes with substituted imidazoles. *Inorg. Chem.* **32**, 2576–2582.

22. Barbucci, R., Bencini, A. & Gatteschi, D. (1977) Electron spin resonance spectra and spin hamiltonian parameters for trigonal-bipyramidal nickel(I) and copper(II) complexes. *Inorg. Chem.* **16**, 2117–2120.

23. Steiner, R.A., Kooter, I.M. & Dijkstra, B.W. (2002) Functional analysis of the copper dependent quercetin 2,3-dioxygenase. 1. Ligand-induced coordination changes probed by X-ray crystallography: inhibition, ordering effects and mechanistic insights. *Biochemistry,* in press.

24. Jurd, L. (1962) Spectral properties of flavonoid compounds. In *The Chemistry of Flavonoid Compounds* (Geissman, T.A., ed.), pp. 107–155. Macmillan, New York.

25. Jovanovic, S.V., Steenken, S., Tosic, M., Marjanovic, B. & Simic, M.G. (1994) Flavonoids as antioxidants. *J. Am. Chem. Soc.* **116**, 4846–4851.

26. Esnouf, R.M. (1997) An exensively modified version of MolScript that includes greatly enhanced coloring capabilities. *J. Mol. Graphics* **15**, 133–138.

27. Merritt, E.A. & Bacon, D.J. (1997) Raster3D: Photorealistic Molecular Graphics. *Methods Enzymol.* **277**, 505–524.